

Similar point defects in crystalline and amorphous silicon

Z. N. Liang and L. Niesen

Nuclear Solid State Physics, Materials Science Center, Groningen University, Nijenborgh 4, 9747 AG Groningen, The Netherlands

G. N. van den Hoven and J. S. Custer

*Fundamenteel Onderzoek der Materie-Institute for Atomic and Molecular Physics,
Kruislaan 407, 1098 SJ Amsterdam, The Netherlands*

(Received 11 November 1993; revised manuscript received 2 February 1994)

The microscopic nature of defects in ion-implanted crystalline silicon (*c*-Si) and amorphous silicon (*a*-Si) has been studied using Mössbauer spectroscopy. The evolution of the local structure around the probe atoms is followed during thermal annealing of ion-beam-created amorphous and ion-beam-damaged crystalline Si. Direct comparison of the Mössbauer parameters of ^{119}Sb in *c*-Si and *a*-Si demonstrates that Sb occupies two distinct sites in each material with similar local environments in both materials. These sites are identified as fourfold-coordinated substitutional Sb and Sb-vacancy complexes. Annealing of ion-beam-damaged *c*-Si at 150°C causes the Sb-vacancy complex to change from a substitutional Sb adjacent to a vacancy to a more complicated complex. Annealing of *a*-Si is shown to reduce distortions in the network, consistent with structural relaxation.

I. INTRODUCTION

Modeling of the amorphous silicon (*a*-Si) network shows the Si atoms to be fourfold coordinated and covalently bonded in a continuous random network.¹ As is generally the case for amorphous systems, the precise structure of *a*-Si depends on the thermal history of the system. Changes in the structure during annealing are called “structural relaxation” and involve an evolution of the system to lower free energies. Structural relaxation and defect annihilation in pure amorphous (*a*-Si) is a subject of many recent studies.^{2–11} Structural relaxation is considered as a process to which every atom in the *a*-Si continuous random network contributes, and has been shown to be mediated or accompanied by annihilation of defects.^{2,10} Similarly, annealing of ion-beam-induced damage in crystalline silicon (*c*-Si) is also mediated by point defect annihilation.² Furthermore, calorimetry studies indicate similar mechanisms for the annealing of defects in *c*-Si and structural relaxation in *a*-Si.² It is known that the amorphous phase can accommodate different types of defects, for instance dangling or floating bonds,¹² or even “frustrated” bonds.¹³ However, these topological defects do not exist *c*-Si. Therefore, the similarities between annealing of *c*-Si and *a*-Si may be understood if point defects similar to those in *c*-Si would also exist in *a*-Si. The aim of the present study is to examine the local environment of impurity atoms in *a*-Si in order to find out if specific impurity-point defect clusters exist similar to those in *c*-Si. Also the evolution during thermal annealing is investigated in detail.

Using Mössbauer spectroscopy it is possible to probe the local environment of a Mössbauer probe atom in a material, yielding information on the electronic, geometric, and magnetic structure.¹⁴ By “local environment,” we primarily mean structure in the volume occupied by the probe atom and its nearest neighbors. The

nuclear energy levels of a probe atom are influenced by the local environment through the hyperfine interaction.¹⁴ The difference in energy levels of the probe nucleus with respect to a reference may be measured by Doppler shifting the probe (or reference) atoms to bring the probe and reference into resonance. The isomer shift δ is then defined as the Doppler velocity at the peak of the resonance, and is a measure of the electron density at the nucleus of the probe atom. The sign of δ is taken as positive if the transition in the probe nucleus has a higher energy than in the reference nucleus. The symmetry of the surroundings may give rise to a splitting of the nuclear energy levels in the probe, due to the interaction between the electric-field gradient and the nuclear quadrupole moment. This results in a quadrupole splitting of the Mössbauer resonance. Furthermore, the vibrational properties of the Mössbauer atoms can be investigated by measuring the recoilless fraction as a function of temperature.

Different techniques have been used to study the lattice location of Sb in *c*-Si. Electron paramagnetic resonance has provided identification of an antimony-vacancy (Sb- V) pair, a neutral complex in which a lattice vacancy sits adjacent to a substitutional Sb atom.¹⁵ Ion channeling and Rutherford backscattering spectrometry (RBS) have been used to measure the displacement of Sb atoms from lattice sites,^{16,17} but are insensitive to the local electronic structures. The combination of channeling and Mössbauer spectroscopy has proven to be very useful for the study of the lattice site location of Sb.¹⁸ Previous Mössbauer studies on ^{119}Sb implanted in *c*-Si show that the Sb atoms can occupy different sites in the lattice.^{18–21} After Sb implantation, Mössbauer spectra generally exhibit two lines, one at $\delta \sim 1.8$ mm/s and one at $\delta \sim 2.3$ – 2.6 mm/s with respect to a reference $\text{Ca}^{119}\text{SnO}_3$ absorber. These lines have been associated with fourfold-coordinated substitutional Sb, and Sb in a vacan-

cy complex, respectively. Subsequent annealing of the crystal at temperatures in the range 600–900 °C leave almost all the Sb atoms on substitutional sites. Furthermore, a line at $\delta = 2.3$ mm/s has been observed for *c*-Si implanted with ^{119}Sb , annealed at 700 °C and subsequently bombarded with α particles.¹⁹ This line was attributed to a substitutional Sb next to a vacancy. Although some data exist on annealing below 600 °C for ion-beam-damaged *c*-Si,^{19,22,23} no extensive annealing studies have been performed. This temperature regime is interesting because many types of point defects become mobile in this range.^{22–26}

The formation of Sb-H complexes in *c*-Si has also been studied using Mössbauer spectroscopy.^{27–30} Crystals implanted with ^{119}Sb , annealed at 900 °C, and subsequently implanted with H_2^+ at 200 eV exhibits two phenomena: (1) a line appears at 2.3 mm/s, attributed to SbH complexes, and (2) the total intensity of the Mössbauer spectrum decreases significantly. This latter phenomenon is attributed to the formation of SbH_2 .³⁰ Both effects disappear after annealing above 175 °C, due to outdiffusion of H.

Using Mössbauer spectroscopy the microscopic nature of defects in *a*-Si has been studied.⁸ Two distinct sites for Sb in *a*-Si were found. Comparison of these sites with those found in *c*-Si demonstrated Sb to occupy substitutional fourfold-coordinated sites and Sb-vacancy complexes in the amorphous phase. Although earlier work^{18,20} has been done in which *c*-Si was implanted with Sb to fluences high enough to amorphize the crystals, in these cases it was not possible to distinguish between contributions from Sb in the crystalline phase or Sb in the amorphous phase.

In this paper, the similarities between structural relaxation in *a*-Si and defect annealing in *c*-Si are studied using $^{119}\text{Sb} \rightarrow ^{119}\text{Sn}$ source Mössbauer spectroscopy. The focus is on *low temperature annealing*, i.e., annealing between room temperature and 600 °C. In *c*-Si containing Sb, point defects were created by H implantation, leading to two lines in the Mössbauer spectrum. These are identified as a substitutional line and a vacancy-associated line. The substitutional line does not change upon annealing, whereas the vacancy-associated line changes in isomer shift at about 150 °C, suggesting the formation of complexes containing more than one vacancy. In *a*-Si, the Mössbauer parameters are very close to those for substitutional Sb and Sb-vacancy complexes in *c*-Si, indicating that similar point defects exist in *c*-Si and *a*-Si. Moreover, the decrease in the linewidth and the splitting of the Mössbauer lines upon annealing indicates structural relaxation, reducing the distortions around the sites of the probe atoms.

II. EXPERIMENTAL PROCEDURES

Radioactive ^{119}Sb is the daughter product of ^{119}Te (half-life 16 h) and ^{119m}Te (half-life 4.7 days) produce in the reaction $^{121}\text{Sb}(p, 3n)^{119(m)}\text{Te}$, using 45 MeV protons from the KVI cyclotron in Groningen. The ^{119}Sb was implanted with an energy of 110 keV using an isotope separator into samples held at room temperature.

For the *c*-Si case, both ^{119}Sb and stable ^{121}Sb were implanted with energies of 110 keV to doses of 1×10^{12} and 5×10^{14} cm^{-2} , respectively, into a $\langle 100 \rangle$ wafer of *p*-type Si (6×10^{15} B cm^{-3}). The crystal was tilted by $\sim 7^\circ$ relative to the beam axis to avoid channeling. Recovery of the implant damage and activation of the Sb was performed by annealing at 900 °C for 30 min in flowing N_2 . The peak concentration of Sb was 5×10^{19} cm^{-3} at about 55 nm as measured by RBS. Point defects were created at room temperature by 9.5-keV hydrogen implantation normal to the sample surface to a dose of 1×10^{16} cm^{-2} . The peak of the hydrogen profile was at about 150 nm, well beyond the Sb profile according to Monte Carlo simulations (TRIM89 [Ref. 31]). Annealing at stepwise increasing temperatures from 100 to 300 °C was carried out in flowing N_2 for 15 min.

Well characterized amorphous Si layers were created by implanting both Czochralski-grown ($\langle 100 \rangle$ *n*-type, 1–20 Ω cm) and a float-zone ($\langle 100 \rangle$ *p*-type, 5–15 Ω cm) *c*-Si with 5×10^{15} 500-keV Si cm^{-2} with the substrate held at 77 K. This resulted in a continuous *a*-Si layer from the surface to a depth of 750 nm as measured by RBS. A low dose ($\sim 10^{12}$ cm^{-2}) of ^{119}Sb ions was implanted at room temperature, with the beam current on target sufficiently low (< 100 pA cm^{-2}) to ensure no beam heating during the implantation. An implantation energy of 110 keV was used, resulting in a projected range of 55 nm, so that all of the ^{119}Sb came to rest within the *a*-Si layer. Structural relaxation of the *a*-Si was induced by annealing at stepwise increasing temperatures from 100 to 550 °C for 15 min in vacuum ($\approx 10^{-6}$ mbar). Subsequently recrystallization of the *a*-Si crystals was carried out by annealing at 600, 700, and 900 °C.

Conversion electron Mössbauer spectroscopy measurements were carried out with the samples held at 80 K, while a reference $\text{Ca}^{119}\text{SnO}_3$ absorber was mounted in an acetone-filled counter that was moved at room temperature using a standard constant acceleration drive.

III. ANTIMONY IN CRYSTALLINE SILICON

A. Results

Figure 1(a) displays the Mössbauer spectrum measured at 80 K for the *c*-Si sample implanted with 5×10^{14} Sb cm^{-2} and annealed at 900 °C for 30 min in flowing N_2 . This spectrum can be analyzed satisfactorily using a single Lorentzian line with an isomer shift δ of 1.78 mm/s and a linewidth 0.85 mm/s. A better fit, as shown by the solid line in Fig. 1(a), was obtained by allowing for a small quadrupole doublet $E_Q = 0.30 \pm 0.05$ mm/s, the linewidth of each component being 0.70 ± 0.02 mm/s. The magnitude of the quadrupole interaction is somewhat dependent on the Sb dose,³² showing that it is partly due to impurity atoms at some distance from the probe. Another part of the quadrupole interaction originates from the $\text{Ca}^{119}\text{SnO}_3$ absorber.²⁷ We denote this line as I_s . The Mössbauer parameters are listed in Table I. This single line indicates that virtually all Sb atoms are on substitutional sites.^{18–21,27}

Figure 1(b) shows the spectrum of the same sample

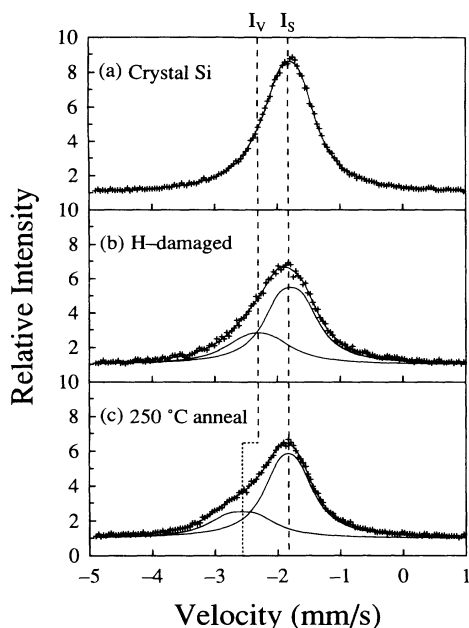


FIG. 1. Conversion electron Mössbauer spectra of *c*-Si taken at 80 K: (a) after implantation with an energy of 110 keV and a dose of 5×10^{14} Sb cm $^{-2}$ and annealing at 900 °C for 30 min in flowing N $_2$; (b) after point defect creation by 9.5 keV hydrogen implantation with a dose of 1×10^{16} cm $^{-2}$ at room temperature; (c) after annealing at 250 °C for 15 min in flowing N $_2$. The solid lines are the least-square fitted results.

after the 1×10^{16} cm $^{-2}$ 9.5-keV H $^+$ implantation, which introduces point defects. It is clear that a second component (denoted by I_v) appears at $\delta = 2.31 \pm 0.09$ mm/s. The relative intensity of this component is about 34%. This line is assigned to an Sb-vacancy complex, as will be discussed later. In addition, the total intensity is slightly lower than in the spectrum before H implantation (see Table I). Annealing the H implanted sample at 250 °C results in the spectrum of Fig. 1(c). A clear change in the isomer shift of I_v is observed, whereas the shape and position of I_s are nearly identical to I_s in Fig. 1(a).

Figure 2(a) shows the relative intensities of I_s and I_v as a function of annealing temperature, resulting from least-square fits to the data with all the parameters free. Only a small change is observed at about 150 °C. The behavior of the isomer shifts is shown in Fig. 2(b). While the isomer shift of I_s stays essentially constant, an increase in the isomer shift of I_v is seen after the 150 °C an-

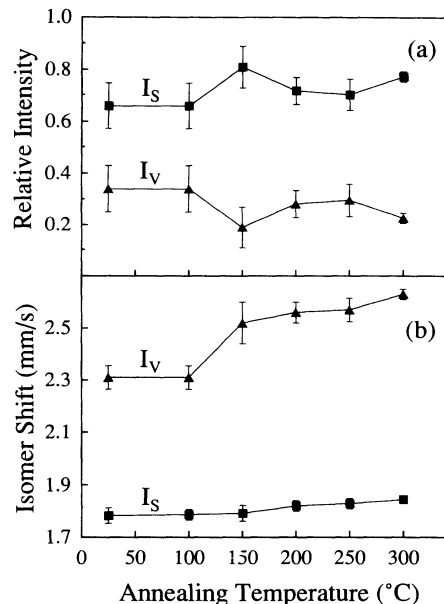


FIG. 2. The Mössbauer parameters as a function of annealing temperature for the *c*-Si sample (see Fig. 1): (a) relative intensity of the substitutional fraction I_s (squares) and the Sb- V complexes I_v (triangles); (b) isomer shifts of I_s and I_v .

nealing. The linewidths and quadrupole splitting for both components are practically constant, independent of annealing temperature.

B. Discussion

The above results show the appearance of two lines, designated by I_s and I_v , in the Mössbauer spectra. Line I_s at $\delta = 1.8$ mm/s has been previously identified as resulting from fourfold-coordinated substitutional Sb. For line I_v (2.3 mm/s) there are two possible candidates: the Sb-vacancy (Sb- V) complex and the Sb-hydrogen (SbH) complex. The Sb- V complex was found in *c*-Si where vacancies were intentionally created,¹⁹ and it is interpreted as due to a simple Sb-vacancy complex, presumably a substitutional Sb atom associated with one vacancy in its near-neighbor shell. The SbH complex arises from hydrogen atoms forming pairs with substitutional Sb in *n*-type *c*-Si, and also leads to a line at 2.30 mm/s.^{28,29} In the present experiment, however, the projected range of the implanted H (150 nm) is well beyond that of the Sb atoms (55 nm). Such H has not been observed to undergo

TABLE I. The Mössbauer parameters obtained by fitting the spectra of the *c*-Si sample with all parameters free.

Parameter	I_s			I_v		
	Before H implant.	After H implant.	250 °C anneal	Before H implant.	After H implant.	250 °C anneal
δ (mm/s)	1.78 ± 0.03	1.79 ± 0.02	1.82 ± 0.02	2.31 ± 0.09	2.57 ± 0.09	2.57 ± 0.09
Linewidth (mm/s)	0.70 ± 0.02	0.71 ± 0.03	0.73 ± 0.02	0.93 ± 0.06	0.86 ± 0.05	0.86 ± 0.05
Splitting (mm/s)	0.31 ± 0.03	0.35 ± 0.02	0.28 ± 0.03	0.39 ± 0.10	0.44 ± 0.10	0.44 ± 0.10
Relative intensity	10.6 ± 0.80	6.25 ± 0.83	6.75 ± 0.48	3.20 ± 0.85	2.63 ± 0.56	2.63 ± 0.56

long-range room-temperature diffusion following implantation,³³ presumably due to the formation of stable bonded configurations. This implies that there is very little H in the range of the Sb profile, whereas the line I_v is already present immediately following implantation. Furthermore, in previous studies explicitly concerned with the formation of Sb-H complexes,^{28,29} the appearance of the Mössbauer line associated with these complexes was always accompanied by a large decrease of the total intensity. As this is not observed here, we can safely assume that the SbH complex has little or no effect on the spectra, and so component I_v (34%) must be predominantly due to the Sb-V complex. The slight decrease in intensity after hydrogen implantation is caused by the fact that the Sb-V complex has a lower Debye temperature (160 ± 20 K) than that of I_s (220 ± 20 K),^{19,21} leading to a lower recoilless fraction for I_v .

Figure 2(b) shows that the isomer shift of line I_s does not change upon annealing, whereas I_v increases from 2.3 to 2.5 mm/s around 150°C. For I_s this implies that the local environment of the substitutional Sb does not change. The fact that I_v changes means that the simple Sb-V complex changes upon annealing at 150°C. It has been shown that divacancies become mobile around this temperature,^{25,26} and may be trapped by substitutional Sb or already existing Sb-V complexes. Using RBS and channeling techniques in particular, Swanson *et al.* have given evidence for the trapping of vacancies by Sb atoms.¹⁶ This trapping reaches a maximum at $\sim 150^\circ\text{C}$. Therefore, the change in the isomer shift of I_v may be indicative of the formation of larger complexes with the general formula Sb- V_n .

In summary, in addition to the fourfold-coordinated substitutional line, we have observed a line corresponding to Sb-vacancy complexes. A single Sb-V complex is the dominant configuration after point defect creation. Subsequent annealing above 150°C gives rise to more complicated clusters, which probably involve more than one vacancy.

IV. ANTIMONY IN AMORPHOUS SILICON

A. Results

Figure 3(a) shows the Mössbauer spectrum of the as-implanted Czochralski-grown (CZ) *a*-Si sample. It can be well fitted using two components: one with $\delta = 1.84 \pm 0.03$ mm/s and one with $\delta = 2.55 \pm 0.09$ mm/s. Table II lists the Mössbauer parameters used to fit each spectrum. Comparison of the *a*-Si isomer shifts to those found for damaged *c*-Si (Table I and Refs. 16 and 19) shows that the line at $\delta = 1.84$ mm/s is very close to that of fourfold-coordinated Sb. Similarly, the line at $\delta = 2.55$ mm/s compares well to the Sb-vacancy complex line found in the damaged *c*-Si. Thus, we will use the same notation for these two lines both in *c*-Si and in *a*-Si, i.e., I_s and I_v .

Annealing at 400°C leads to small changes of the Mössbauer parameters for the *a*-Si sample, as can be seen from Fig. 3(b) and Table II. While the isomer shifts are more or less the same as the as-implanted sample, the

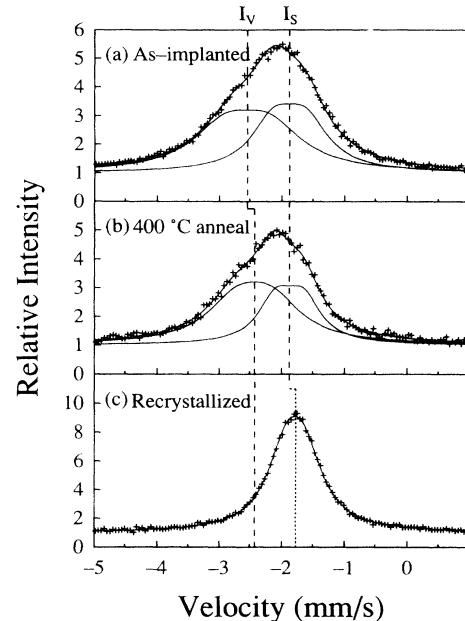


FIG. 3. Conversion electron Mössbauer spectra for the CZ *a*-Si taken at 80 K of ^{119}Sb in *a*-Si (a) as implanted, (b) after annealing at 400°C for 15 min in vacuum which induces structural relaxation, and (c) after recrystallization at 600°C. The lines are the least-square fits to the data.

linewidths become narrower. The results for the float-zone *a*-Si are similar (not listed), indicating that low levels of other impurities (e.g., O and C) do not influence the results.

The linewidths and quadrupole splitting of I_s and I_v as a function of annealing temperature are shown in Fig. 4. Because the isomer shifts of both I_s and I_v are constant within the error bars, the spectra were fitted with the same values for the isomer shifts. These Mössbauer parameters were obtained from an optimization procedure in which all the spectra were fitted at the same time. This procedure yields isomer shifts of 1.87 and 2.44 mm/s for I_s and I_v , respectively. Figure 4 shows that the linewidths and the splitting of both I_s and I_v become smaller upon annealing. Annealing at 600°C results in complete solid phase epitaxy of the *a*-Si, transforming it to *c*-Si, and Fig. 3(c) indeed shows the narrow single line at $\delta = 1.8$ mm/s expected for *c*-Si.

The relative intensities of the Mössbauer lines are displayed in Fig. 5 as a function of annealing temperature. The relative intensity of I_v remains more or less unchanged for annealing temperatures up to 550°C and then disappears completely upon annealing at 600°C, where recrystallization occurs. Moreover, part of the substitutional intensity vanishes gradually after successive annealing steps. After recrystallization at 600°C, the total Mössbauer intensity is recovered in the form of a single narrow line.

B. Discussion

The Mössbauer spectra of Sb in *a*-Si (Fig. 3) essentially show the same two lines as found in *c*-Si. In *c*-Si, these

TABLE II. The Mössbauer parameters obtained by fitting the spectra of the CZ *a*-Si sample with all parameters free.

Parameter	I_s			I_v		
	as-implanted <i>a</i> -Si	400 °C anneal	600 °C anneal	as-implanted <i>a</i> -Si	400 °C anneal	600 °C anneal
δ (mm/s)	1.84±0.03	1.85±0.02	1.79±0.01	2.55±0.09	2.43±0.08	
Linewidth (mm/s)	0.87±0.05	0.71±0.07	0.74±0.01	1.31±0.05	1.18±0.06	
Splitting (mm/s)	0.43±0.02	0.42±0.03	0.29±0.01	0.46±0.10	0.51±0.11	
Relative intensity	4.99±0.87	2.84±0.70	10.8±0.10	5.22±0.90	5.26±0.76	

lines were identified as originating from Sb on a fourfold-coordinated substitutional site and Sb in a vacancy-associated complex. The data presented here are in perfect agreement with our previous work,⁸ in which we showed that comparison of the published *c*-Si spectra with the data found for *a*-Si strongly suggests the same type of environment of Sb in *a*-Si. This implies that the concept of impurity-vacancy complexes also applies to *a*-Si. It strongly supports the idea that vacancy-type point defects are generally present in *a*-Si.

Comparison of Mössbauer parameters found for *a*-Si to those of *c*-Si (Tables I and II) shows that the linewidths of I_s and I_v are significantly larger in the amorphous case. Also the quadrupole splitting of I_s is larger for *a*-Si. In addition, Fig. 4 shows that the linewidths and quadrupole splitting found in *a*-Si decrease upon annealing, an effect not seen in *c*-Si. The Mössbauer linewidth and quadrupole splitting may be influenced in several ways. First of all, bond-angle distortion may lead to slightly different hybridizations and, therefore, different electron densities at the nucleus, giving rise to slightly different isomer shifts. This will, in general, broaden the Mössbauer line.

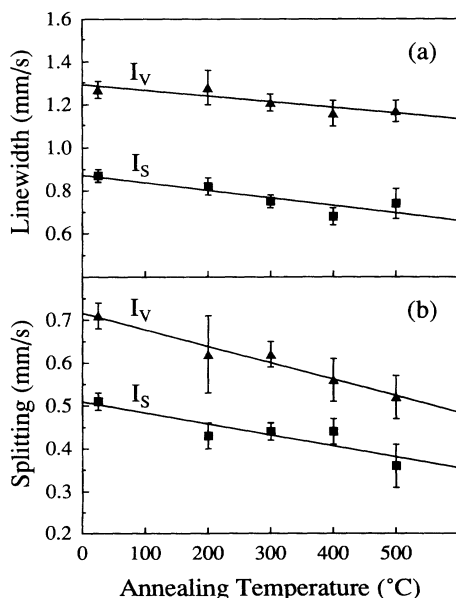


FIG. 4. The linewidth (a) and quadrupole splitting (b) of I_s (squares) and I_v (triangles) as a function of annealing temperature for the CZ *a*-Si sample. The least-square fits to the data are shown with solid lines.

Second, bond-angle distortion and other defects will produce an electric-field gradient at the Sb(Sn) nucleus, leading to a quadrupole splitting of the line. Finally, the local environment around the probe may be different from site to site, leading to a distribution of isomer shifts and quadrupole splittings. Effectively this will again lead to a broadening of the lines.

In general, many physical properties of *a*-Si depend on the preparation conditions and subsequent thermal treatment.² Variations in the material properties of *a*-Si can be mainly attributed to variations in bond-angle distortion or to variations in the density of small voids, dangling or floating bonds, and other types of defects.² The fact that the Mössbauer linewidths for *a*-Si are significantly larger than for *c*-Si implies that there is significant bond-angle distortion around the sites of Sb in *a*-Si. This is not surprising, as it is also observed for the Si network itself. Note that these effects occur not only for the substitutional site but also for the vacancy complex.

Annealing of the as-implanted *a*-Si network results in structural relaxation,^{2,3} which is observed here as a reduction in linewidths and quadrupole splitting with annealing temperature. More specifically this means that the bond-angle distortions and site-to-site variations decrease. These effects are consistent with the decrease in bond-angle deviations upon structural relaxation observed by Raman spectroscopy.⁵ For ion-beam-damaged *c*-Si these changes are absent, implying an absence of

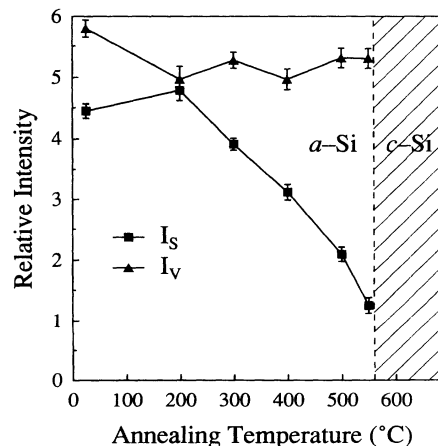


FIG. 5. Relative intensities of I_s and I_v as a function of annealing temperature for the CZ *a*-Si sample. At 600 °C the total intensity is recovered to be 10.8±0.1, see Table II.

large bond-angle distortions and site-to-site variations in the surroundings of the atoms. This means that the displacements created by H implantation in *c*-Si results in simple point defects.

The average isomer shift found for the fourfold-coordinated substitutional line in *a*-Si is 1.87 mm/s, which is slightly higher than that in *c*-Si. This is probably due to bond bending in the *a*-Si network, which may lead to slightly different hybridizations than in the ideal sp^3 hybridization. This gives rise to different electron charge density at the Sb(Sn) nucleus, reflected by the increase of ~ 0.05 – 0.1 mm/s in isomer shift from *c*-Si to *a*-Si. For the vacancy-associated component we observe an average isomer shift $\delta = 2.44$ mm/s. This may be compared with the values for *c*-Si: $\delta = 2.31$ mm/s for the monovacancy line and $\delta = 2.57$ mm/s for the multivacancy component.

Figure 5 shows that the relative intensity of the defect complex (I_v) is more or less constant during annealing below 550°C. This suggests that the Sb-*V* complexes are stable up to 550°C. However, the intensity of the substitutional line (I_s) decreases significantly between 200 and 550°C. This suggests that substitutional Sb atoms change their location to a site in which the ^{119}Sn atoms created in the decay of ^{119}Sb have a large displacement during the Mössbauer decay, destroying the Mössbauer effect. Such an “invisible” fraction has been observed earlier^{28,30} in a system of Sb-hydrogen pairs in *n*-type *c*-Si, where it was shown to grow mainly at the cost of the substitutional component and was attributed to an Sb atom associated with two (or more) H atoms.³⁰ Although H was not introduced on purpose in this case, we cannot exclude H trapping by Sb atoms during the cooling phase of the annealing procedure. Incorporation of H in *a*-Si is known to occur even during vacuum annealing,³⁴ and has a marked influence on the solid phase epitaxy rate. However, in our opinion this is but one of the many possibilities, and a more convincing explanation of the intriguing “invisible” fraction has yet to be made.

In summary, Sb in *a*-Si occupies the same two sites as in *c*-Si, namely the fourfold-coordinated substitutional

site and the Sb-vacancy complex. Annealing of as-implanted *a*-Si gives evidence for structural relaxation as inferred from the reductions in linewidths and quadrupole splitting. Naturally, these effects are absent in ion-beam-damaged *c*-Si with a low level of defects, in which structural relaxation does not take place.

V. CONCLUSIONS

Mössbauer spectroscopy of ^{119}Sb in *c*-Si and *a*-Si demonstrates that Sb occupies two distinct sites in these materials. These sites are identified as fourfold-coordinated substitutional Sb, and Sb-vacancy complexes. The results provide evidence that analogous point defects exist in *c*-Si and *a*-Si, and strongly suggest that vacancies also exist in *a*-Si.

In ion-beam-damaged *c*-Si the Sb-vacancy complex consists of a substitutional Sb with a vacancy in its nearest-neighbor shell. Annealing at $\geq 150^\circ\text{C}$ causes evolution of this complex to a more complicated one, probably involving more than one vacancy. Annealing of as-implanted *a*-Si causes structural relaxation, reducing the distortions in the *a*-Si network as obvious from the reduction of a quadrupole splitting. During this annealing the local environment of the vacancy-associated component is nearly constant, while part of the substitutional Sb atoms find sites in which they undergo such large displacement after the decay to ^{119}Sn that they are invisible in the Mössbauer measurement. Annealing at 600°C leads to solid phase epitaxy, after which all Sb atoms are found at substitutional sites.

ACKNOWLEDGMENTS

We acknowledge the help of F. Th. ten Broek, J. J. Smit, and the crew of the KVI cyclotron during various stage of the experiments. This work is part of the research program of the Foundation for Fundamental Research on Matter (FOM) with financial support from the Dutch Organisation for the Advancement of Pure Research (NWO).

¹D. E. Polk, *J. Non-Cryst. Solids* **5**, 365 (1971).

²S. Roorda, W. C. Sinke, J. M. Poate, D. C. Jacobson, S. Dierker, B. S. Dennis, D. J. Eaglesham, F. Spaepen, and P. Fuoss, *Phys. Rev. B* **44**, 3702 (1991), and references therein.

³S. Roorda, S. Doorn, W. C. Sinke, P. M. L. O. Scholte, and E. van Loenen, *Phys. Rev. Lett.* **62**, 1880 (1989).

⁴E. P. Donovan, F. Spaepen, J. M. Poate, and D. C. Jacobson, *Appl. Phys. Lett.* **55**, 1516 (1989).

⁵C. N. Waddell, W. G. Spitzer, J. E. Fredrickson, G. K. Hubler, and T. A. Kennedy, *J. Appl. Phys.* **55**, 4361 (1984).

⁶W. C. Sinke, T. Warabisako, M. Miyao, T. Tokuyama, S. Roorda, and F. W. Saris, *J. Non-Cryst. Solids* **99**, 308 (1988).

⁷S. Roorda, J. M. Poate, D. C. Jacobson, D. J. Eaglesham, B. S. Dennis, W. C. Sinke, and F. Spaepen, in *Beam-Solid Interactions: Physical Phenomena*, edited by J. A. Knapp, P. Borghesen, and R. A. Zuh, *MRS Symposia Proceedings No. 157* (Materials Research Society, Pittsburgh, 1990), p. 683.

⁸G. N. van den Hoven, Z. N. Liang, L. Niesen, and J. S. Custer, *Phys. Rev. Lett.* **68**, 3714 (1992); **70**, 2197 (1993).

⁹W. C. Sinke, S. Roorda, and F. W. Saris, *J. Mater. Res.* **3**, 1201 (1988).

¹⁰P. A. Stolk, L. Calcagnile, S. Roorda, W. C. Sinke, A. J. M. Bernsten, and W. F. van der Weg, *Appl. Phys. Lett.* **60**, 1688 (1992).

¹¹S. Roorda, J. S. Custer, W. C. Sinke, J. M. Poate, D. C. Jacobson, A. Polman, and F. Spaepen, *Nucl. Instrum. Methods Phys. Res. B* **59/60**, 344 (1991).

¹²S. T. Pantelides, in *Fundamentals of Beam-Solid Interactions and Transient Thermal Processing*, edited by M. J. Aziz, L. E. Rehn, and B. Stritzker, *MRS Symposia Proceedings No. 100* (Material Research Society, Pittsburgh, 1988), p. 387.

¹³S. T. Pantelides, *Solid State Commun.* **84**, 221 (1992).

¹⁴D. L. Williamson *et al.*, in *Hyperfine Interaction of Defects in Semiconductors*, edited by G. Langouche (Elsevier, Amster-

- dam, 1992), p. 1.
- ¹⁵E. L. Elkin and G. D. Watkins, *Phys. Rev.* **174**, 881 (1968).
- ¹⁶M. L. Swanson, J. A. Davies, A. F. Quenneville, F. W. Saris, and L. W. Wiggers, *Radiat. Eff.* **35**, 51 (1978).
- ¹⁷F. W. Saris, in *Defects and Radiation Effects in Semiconductors*, edited by R. R. Hasiguti, IOP Conf. Proc. No. 59 (Institute of Physics and Physical Society, London, 1981), p. 111.
- ¹⁸A. Nylandsted-Larsen, F. T. Pedersen, G. Weyer, R. Galloni, R. Rizzoli, and A. Armigliato, *J. Appl. Phys.* **59**, 1908 (1986).
- ¹⁹S. Damgaard, J. W. Petersen, and G. Weyer, *Hyperfine Interact.* **10**, 751 (1981).
- ²⁰G. Weyer, S. Damgaard, J. W. Petersen, and J. Heinemeier, *Nucl. Instrum. Methods Phys. Res.* **199**, 441 (1982).
- ²¹G. Weyer, A. Nylandsted Larsen, N. E. Holm, and H. L. Nielsen, *Phys. Rev. B* **21**, 4939 (1980).
- ²²M. Hirata, M. Hirata, H. Saito, and J. H. Crawford, Jr., *J. Appl. Phys.* **38**, 2433 (1967).
- ²³M. Hirata, M. Hirata, and H. Saito, *J. Phys. Soc. Jpn.* **27**, 405 (1969).
- ²⁴C. S. Nichols, C. G. Van de Walle, and S. T. Pantelides, *Phys. Rev. B* **40**, 5484 (1989).
- ²⁵F. L. Vook and H. J. Stein, *Radiat. Eff.* **2**, 23 (1969).
- ²⁶F. L. Vook, in *Radiation Damage and Defects in Semiconductors*, edited by J. E. Whitehouse, IOP Conf. Proc. No. 16 (Institute of Physics and Physical Society, London, 1973), p. 60.
- ²⁷Z. N. Liang and L. Niesen, *Hyperfine Interact.* **60**, 749 (1990).
- ²⁸Z. N. Liang and L. Niesen, *Mater. Sci. Forum* **83-87**, 99 (1992).
- ²⁹Z. N. Liang and L. Niesen, *Nucl. Instrum. Methods Phys. Res. Sect. B* **63**, 147 (1992).
- ³⁰Z. N. Liang, C. Haas, and L. Niesen, *Phys. Rev. Lett.* **72**, 1846 (1994).
- ³¹J. P. Biersack and L. G. Haggmark, *Nucl. Instrum. Methods* **174**, 257 (1980).
- ³²Z. N. Liang and L. Niesen (unpublished).
- ³³G. F. Cerofolini, L. Meda, C. Volpones, G. Ottaviani, J. DeFayette, R. Dierckx, D. Donelli, M. Orlandini, M. Anderle, R. Canteri, C. Claeys, and J. Vanhellefont, *Phys. Rev. B* **41**, 12 607 (1990).
- ³⁴J. A. Roth, G. L. Olson, D. C. Jacobson, J. M. Poate, and C. Kirschbaum, in *Kinetics of Phase Transformations*, edited by M. O. Thompson, M. Aziz, and G. B. Stephenson, MRS Symposia Proceedings No. 205 (Materials Research Society, Pittsburgh, 1992), p. 45.